sociedade & natureza

DOI: 10.14393/SN-v35-2023-67666x
Receveid: November 30, 2022 | Accepted: April 10, 2023 | Published: June 19, 2023

Papers

Mapping of aridity and its connections with climate classes and climate desertification in future scenarios – Brazilian semi-arid region

Lucas Augusto Pereira da Silva[1]
Claudionor Ribeiro da Silva[2]
Cristiano Marcelo Pereira de Souza[3]
Édson Luis Bolfe[4]
João Paulo Sena Souza[5]
Marcos Esdras Leite[6]

Keywords
Spatial modeling
Semi-arid zone
Droughts
Climate change

Abstract
Brazil has the most populous and biodiverse semi-arid region in the world (Brazilian Semi-arid - SAB). However, in recent decades, clusters of desertification have emerged, a problem that could intensify from climate change. The objective of this study was to elaborate on the spatial distribution of areas susceptible to climatic desertification in the SAB, considering future climate change scenarios. Understanding this dynamic is essential for SAB's agri-environmental management. Aridity indices and proposition of climate classes for current condition (1970-2000) and future scenarios (2061-2080) of the Intergovernmental Panel on Climate Change (IPCC) were prepared, considering scenarios from Shared Socioeconomic Pathways: Optimistic (SSP 126) and pessimists (SSP 585). The results indicate that by the end of the century, the climate in the SAB should become significantly drier (Kruskal-Wallis = p-value < 0.05), with an intensification of the aridity index in SSP 585. In the scenarios, the expansion of more arid areas over humid climates could reach 56,500 km² (10%) in SSP 126 and 140,400 km² (24%) in SSP 585. Consequently, areas with high (622,400 km² to 706,300 km²) and very high (622,400 km² to 706,300 km²) are expected to expand. 4,400 to 21,700 km²) susceptibility to climate desertification in the SAB, respectively in scenarios SSPs 126 and 585. Confirming these projections would imply socioeconomic and ecological risks in the SAB.

[1] Universidade Federal de Uberlândia - UFU, Uberlândia, MG, Brazil. lucaskaio1605@gmail.com
[2] Universidade Federal de Uberlândia - UFU, Uberlândia, MG, Brazil. crs@ufu.br
[3] Universidade Estadual de Montes Claros - UNIMONTES, Montes Claros, MG, Brazil. souzacristianomp@gmail.com
[4] Empresa Brasileira de Pesquisa Agropecuária - Embrapa e Universidade Estadual de Campinas – UNICAMP, Campinas, SP, Brazil. edson.bolfe@embrapa.br
[5] Universidade Estadual de Montes Claros - UNIMONTES, Montes Claros, MG, Brazil. jpsenasouza@gmail.com
[6] Universidade Estadual de Montes Claros - UNIMONTES, Montes Claros, MG, Brazil. marcos.leite@unimontes.br

INTRODUCTION

The semi-arid regions cover approximately 40% of the Earth's surface, and host more than 14% of the world's population (HUANG et al., 2016). These areas are essential for the global economy and ecology, supplying many ecosystem services (WU et al., 2021). Despite their importance, semi-arid regions are extremely sensitive to the effects of climate change, leading to desertification processes (BURRELL et al., 2020). Therefore, understanding the climatic variables in future scenarios is essential for managing semi-arid regions.

Desertification in semi-arid zones is a global problem that disproportionately affects the world's poorest areas (POZO et al., 2019). Conceptually, desertification is a complex phenomenon resulting from the interaction of natural and anthropogenic factors that affect arid, semi-arid, and dry sub-humid areas (MMA, 2004). Climate desertification is a subset of desertification that specifically refers to changes in certain climate variables (UNEP, 1992). Both forms of desertification involve decreased precipitation, increased air temperature, and increased potential evapotranspiration (ZHOU et al., 2021). All those changes potentially increase aridity, an index of the degree of dryness of these environments (ZARCH et al., 2017).

By the end of the century, the aridity in semi-arid regions is expected to intensify, amplifying the already prevalent dryness in these areas. (HUANG et al., 2016), according to projections formulated by the Intergovernmental Panel on Climate Change (IPCC). If confirmed, this trend will lead to changes in weather conditions characterized by decreasing humidity that may cause desertification (ZARCH et al., 2017). The process of desertification has several negative impacts, including the disruption of socioeconomic flows, heightened levels of poverty, and increased rates of migration among both animal and human populations (HUANG et al., 2016; SANZHEEV et al., 2020). Desertification also reduces land productivity, causes soil loss, increases CO_2 rates, and declines biodiversity levels (HUANG et al., 2016). Therefore, it is crucial to monitor the progress of this process, especially in semi-arid areas, in order to mitigate local socioeconomic and environmental problems of local and global dimensions.

South America is one of the most affected regions by desertification processes. About 10% (~200 million hectares) of the continent's lands presents some degree of degradation, with a tendency to worsen in future scenarios (VERGARA et al., 2015). The Brazilian semi-arid region (SAB) is inserted in this context, with more than twenty-eight million inhabitants (IBGE, 2010), constituting the most populous semi-arid zone in the world.

The SAB has high biodiversity, with the presence of the Caatinga biome (with xerophytic vegetation), and enclaves of Cerrado (semi-deciduous characteristics), and Atlantic Forest (ombrófila vegetation) that create unique ecosystems (AB'SABER, 2003). Additionally, it has anthropic uses of substantial socioeconomic importance. However, recent studies show an increase in areas of desertification, ecological succession of plant species more adapted to drought, and intensification of socioeconomic problems (MARQUES SILVA et al., 2018; CASTRO OLIVEIRA et al., 2021).

Recent studies show the impacts of climate change on the spatial distribution of desertification-susceptible areas in the SAB (MARQUES DA SILVA et al., 2018; VIEIRA et al., 2020). However, the number of studies that analyze future climate conditions, especially on an adequate scale, are few (VIEIRA et al., 2021). Additionally, new analysis techniques have been used for climate variable studies in desertification research, such as the use of machine learning algorithms in modeling (FENG et al., 2022). One advantage of this methodological structure is the inclusion of environmental covariates in modeling. Covariates help explain the spatial distribution of the variable and increase the accuracy of spatial models (SILVA et al., 2023). Therefore, this study aims to evaluate the spatial distribution of areas susceptible to climatic desertification considering the effects of future climate change scenarios (2061-2080). Additionally, maps of aridity index (AI) and climate classes were created to achieve this goal for future scenarios.

MATERIALS AND METHODS

Study area

The SAB is located in the northeastern portion of South America, between 0° and 20° South latitude (Figure 1d, e). The region encompasses 13% of the Brazilian territory, including states in the Northeast region and part of the northern state of Minas Gerais.

The SAB region is influenced by atmospheric systems such as cold fronts from the southeastern Brazil region and seasonal variations of the Inter-Tropical Convergence Zone (MUTTI et al., 2020). The air temperature has high average values (up to 27 °C) recorded in the northwestern portion. The lowest averages (19-21°C) prevail on the eastern edge, where the arrival of moist fronts from the ocean is more constant (Figure 1a).

Figure 1 - SAB Location. A) Spatial distribution of average air temperature (1970-2000). B) Annual precipitation. C) Potential evapotranspiration using the Penman-Monteith method (ETo-PM). D) SAB boundary. E) SAB in the world.

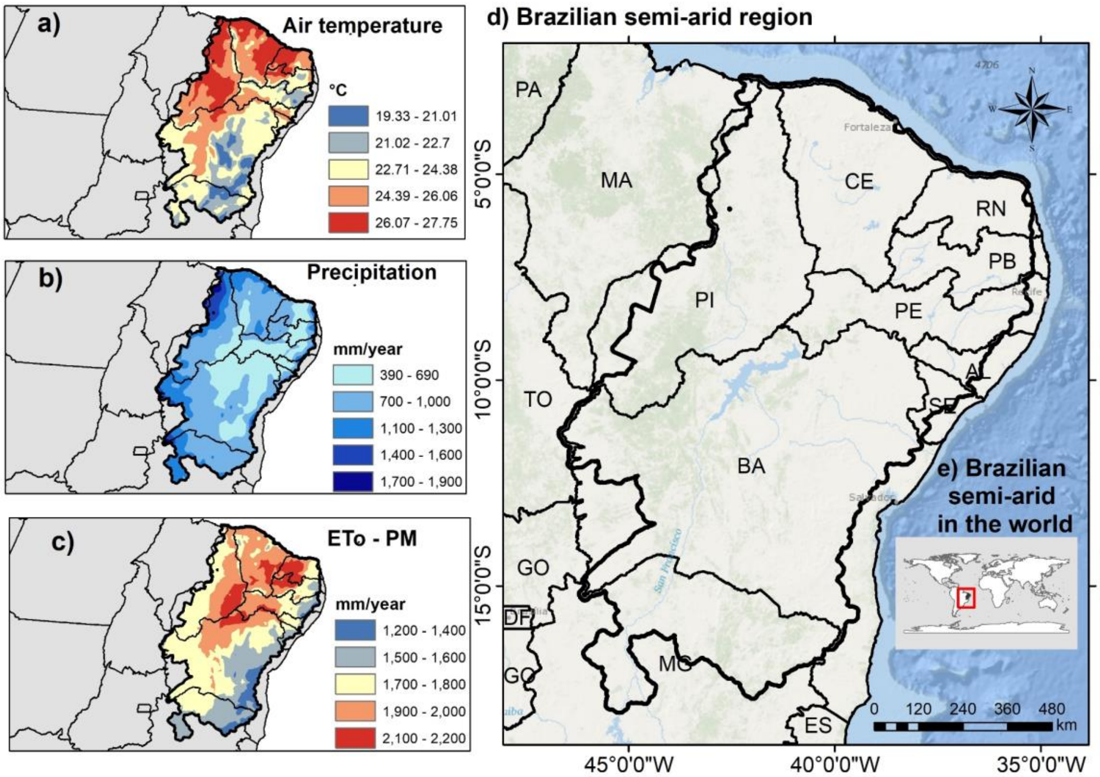

Source: The authors (2023).

The SAB region presents an irregular rainfall distribution throughout the year, characterized by a dry period during the winter. Some parts may have precipitation levels as low as 290 mm during this period. The lowest precipitation occurs in the middle area (390-690 mm/year), while the highest occurs on the eastern edge and the northwest portion (1700-1990 mm/year).

Potential evapotranspiration is higher in the central portion (1200-2200 mm/year), where solar radiation levels are intense. Furthermore, the effect of moist fronts is reduced, and there are lower levels of precipitation (Figures 1b, c).

METHODOLOGICAL PROCEDURES

Aridity Index (current and future)

The AI was obtained using the Thornthwaite method (1948), calculated by the ratio between rainfall (*P*) and potential evapotranspiration (*ETo*) (Equation 01). The lower the AI, the drier the land, while higher values represent more humid environments. The AI was calculated for both current (1970-2000) and future scenarios (2061-2080). Rainfall and evapotranspiration data compatible with these periods were generated.

$$\boldsymbol{AI} = \frac{\boldsymbol{P}}{\boldsymbol{ETo}} \qquad \text{(Equation 1)}$$

Where P and ETo represent annual precipitation and potential evapotranspiration, respectively.

Precipitation (Current and Future Scenarios)

The precipitation data used to build the AI were from worldclim 2.1 products that have a spatial resolution of 10 km, available for current conditions (1970-2000) and future scenarios (2061-2080) (FICK et al., 2017).

Future precipitation data were based on information from global climate change scenarios from the Intercompared Project 6 Coupled Model (CMIP6). CMIP6 establishes climate scenarios ranging from ambitious mitigation to continuous growth in greenhouse gas emissions.

The scenarios projected by CMIP6 are called The Shared Socio-Economic Pathways (SSPs). This research selected the SSPs representing future global socioeconomic trajectories of mitigation (SSP126) and increasing emissions (SSP585). Therefore, in SSP126, it is projected that CO_2 levels will decline by 2050, with a 1.8 °C temperature increase (optimistic scenario). SSP585 describes a future where no significant climate policies and economic and population growth remain the main priorities, standing for a scenario of high greenhouse gas emissions.

Each SSP has projections of climate data based on General Circulation Models (GCMs). GCMs supply climate and bioclimatic variables for future scenarios (Table 1). However, to reduce the effect of uncertainties, a recommended procedure in the literature is calculating the mean of the climate and bioclimatic variables present in the GCMs (HAUSFATHER et al., 2022). Therefore, the precipitation data from SSP126 and SSP585 scenarios were obtained from the mean of five atmospheric circulation models (INM-CM4-8, INM-CM5-0, MIROC6, GISS-E2-1-H, and MIROC-ES2L). The mean procedure was also applied to bioclimatic variables, which were used to assist in modeling the ETo variable.

Table 1 – Climatic and bioclimatic variables for current conditions (1970 – 2000) and future scenarios (2061 – 2080).

Abbreviation	Variables of current and future scenarios	Abbreviation	Variables of current and future scenarios
Bio 01	Annual Mean Temperature	Bio 11	Mean Temperature of Coldest Quarter
Bio 02	Mean Diurnal Range	Bio 12	Annual Precipitation
Bio 03	Isothermality	Bio 13	Precipitation of Wettest Month
Bio 04	Temperature Seasonality	Bio 14	Precipitation of Driest Month
Bio 05	Max Temperature of Warmest Month	Bio 15	Precipitation Seasonality
Bio 06	Min Temperature of Coldest Month	Bio 16	Precipitation of Wettest Quarter
Bio 07	Temperature Annual Range	Bio 17	Precipitation of Driest Quarter
Bio 08	Mean Temperature of Wettest Quarter	Bio 18	Precipitation of Warmest Quarter
Bio 09	Mean Temperature of Driest Quarter	Bio 19	Precipitation of Coldest Quarter
Bio 10	Mean Temperature of Warmest Quarter	SRTM	Altitude

Source: Fick et al. (2017).

Evapotranspiration ET0 (Current and Future Scenarios)

The potential evapotranspiration was obtained from the EToBrasil dataset (ALTHOFF et al., 2020). This is a dataset modeled by machine learning algorithms. These data were chosen because they have a low density of weather stations in the SAB.

The temporal scale of the EToBrasil data is daily from 2000 to 2020, with a spatial resolution of 10 km. To equalize the temporal range of ETo (2000-2020) with the current (1970-2000) and future (2061-2080) precipitation data, new ETo modeling using machine learning algorithms was performed for the current and future scenarios.

In the ETo modeling, the input data considered the daily average over 20 years (2000-2020), obtained from 6,827 images from the EToBrasil database. The sampling of values consisted of creating a grid of 2,056 points randomly distributed in the SAB, minimum distance between points of 10 km.

The next stages were performed in an R programming language environment (TEAM, 2022). The modeling steps of current and future ETo data were helped by a dataset of climatic and topographic covariates (Table 1). The covariates used were nineteen bioclimatic variables from WorldClim, available for current conditions (1970-2000) and future scenarios (2061-2080) – (Table 1). A topographic covariate was inserted based on the SRTM digital elevation model. Altitude was used because it alters the spatial distribution patterns of ETo rates (LIU et al., 2021).

From the sample data (2,056 points), a regression matrix of the variable *y* (ETo) was created, and the values of the covariates were extracted (Table 1). This regression matrix was elaborated into three sets of covariates encompassing current climate conditions and two future climate scenarios (SSP 126 and SSP 585) (Table 1).

The correlation level between the covariates inserted in the regression matrix was analyzed using the findcorrelation function to discard highly correlated covariates that can generate overestimated results in modeling (SOUZA et al., 2018). The criterion used was the Spearman coefficient to search for covariates with a correlation level above 0.95.

Subsequently, each regression matrix was divided into two sets, training (75%) and testing (25%). Finally, five machine learning models were selected to predict current and future ETo (Table 2). The models were trained with 75% of the samples, using cross-validation. The remaining 25% was used for external validation and selection of the model with the best performance, i.e., > R-squared (R^2) and < Root Mean Square Error (RMSE).

Table 2 – Machine learning algorithms used to train and predict potential evapotranspiration in current and future scenarios.

Machine learning models	Source/Package
Cubist	(KUHN; QUINLAN, 2018)
Random Forest	(LIAW; WIENER, 2002)
Bayesian regularized neural networks	(RODRIGUEZ; GIANOLA, 2016)
Multivariate Adaptive Regression Splines	(MILBORROW; TIBSHIRANI, 2019)
Linear regression	(TEAM, 2022)

Aridity index, spatial distribution and statistical analyzes

Based on the modeled ETo variable for current and future conditions, along with current (1970-2000) and future (2061-2080) precipitation data obtained by averaging GCMs, the Aridity index (AI) was calculated (Equation 01). Thresholds of the AI were used for climatic classification and spatial distribution of areas susceptible to desertification in the SAB. The criteria followed were the recommendations of the World Atlas of Desertification (UNEP, 1992) (Table 3).

Tabela 1 – Climatic classification and levels of susceptibility to desertification as a function of the Thornthwaite aridity index (1948)

Climatic classes	Desertification susceptibility	Aridity Index
Arid	Very High	0,05 < 0,20
semi-arid	High	0,21 < 0,50
dry subhumid	Moderate	0,51 < 0,65
humid subhumid	Moderate	> 0,65

Source: Thornthwaite (1948); UNEP (1992).

Simple linear regressions were performed to understand how precipitation and ETo affect aridity levels under current and future conditions. In addition, the Kruskal-Wallis test was used to evaluate whether there were significant changes in aridity index values in response to climate change scenarios. The spatial distribution of aridity classes was analyzed using Sankey diagrams created with the ggplot2 alluvial package in R (BRUNSON, 2020).

RESULTS

Algorithms performance in the prediction of ETo

The regression matrix for predicting ETo was initially constructed with 20 covariates, however, after applying findcorrelation, four covariates were removed due to correlation > 0.95 (Bio2, Bio11, Bio16, and Bio17 – Table 1).

Regarding statistical validation, the Cubist and RF algorithms performed better (R^2 = 0.97 and 0.98, RMSE = 0.07 and 0.08 mm day^{-1}, respectively). The BRNN presented intermediate metrics between the algorithms. Earth and LM had the worst performance for predicting ETo in the SAB (Figure 2). Cubist was selected to predict ETo because it had better metrics than RF.

Figure 2 – External validation for BRNN (regularized Bayesian neural networks), Cubist, Earth, LM (linear regression) and RF (Random Forest). Figure 2a) Boxplot of R^2 and Figure 2b) Boxplot of RMSE (Square Root Mean Error)

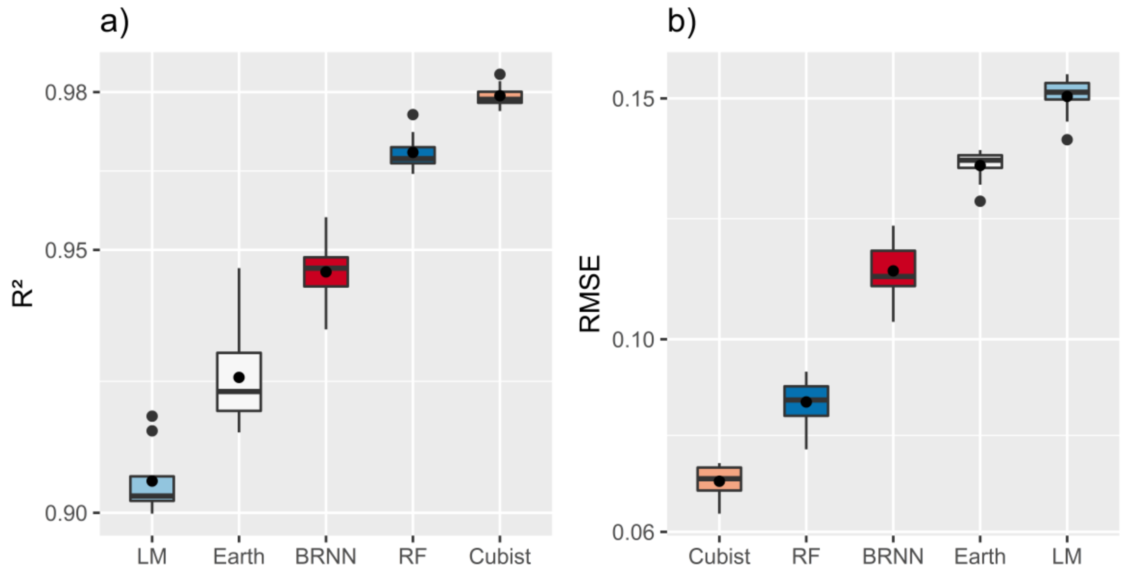

Source: The authors (2023).

Aridity Index (IA): current conditions (1970 – 2000) and future scenarios (2061 – 2080)

Until the end of the century, the SAB region will become significantly drier with an intensification of aridity (Thornthwaite aridity index) (Kruskal-Wallis p-value <0.05). In the current scenario, the average AI in the SAB was 0.49, a typical value for a semi-arid region (Table 3). In the optimistic climate change scenario (SSP 126), a 6% decrease is projected compared to the current average. In the pessimistic scenario (SSP 585), a 14% reduction is expected, both showing an intensification of aridity.

Areas with higher aridity are more susceptible to climate desertification (Table 3) and are expected to expand territorially in response to climate change. The AI value of 0.33, standing for a high susceptibility to climate desertification, showed an expansion of 46,000 km² (+29%) in SSP 126 and 125,600 km² (+79%) in SSP 585. The region where these AI values prevail is in the central part of the SAB, where there are also projections of the recurrence of lower annual precipitation levels (~590 mm) and higher ETo levels (~2,300 mm) (Figure 3). Regression analyses confirmed these relationships (Figure 4), especially for rainfall (R^2>0.87).

The expansion of arid lands (AI between 0.34 and 0.53) in future scenarios was also seen in the southern portions of the SAB. This expansion is worrying because, in the current scenario, more humid conditions are prevailing (dry sub-humid, humid sub-humid), with AI ranging from 0.54 to 0.65 (moderate susceptibility to desertification). The inversion of this situation should be induced by the expansion of zones with higher ETo values (1,900 and 2,200 mm) and lower precipitation levels (600-830 mm) (Figure 3).

Figure 3 - Spatial distribution of the aridity index (AI), annual precipitation and potential evapotranspiration (ETo) for the Brazilian semi-arid region under current conditions (1970 – 2000) and future scenarios (2061 – 2080)

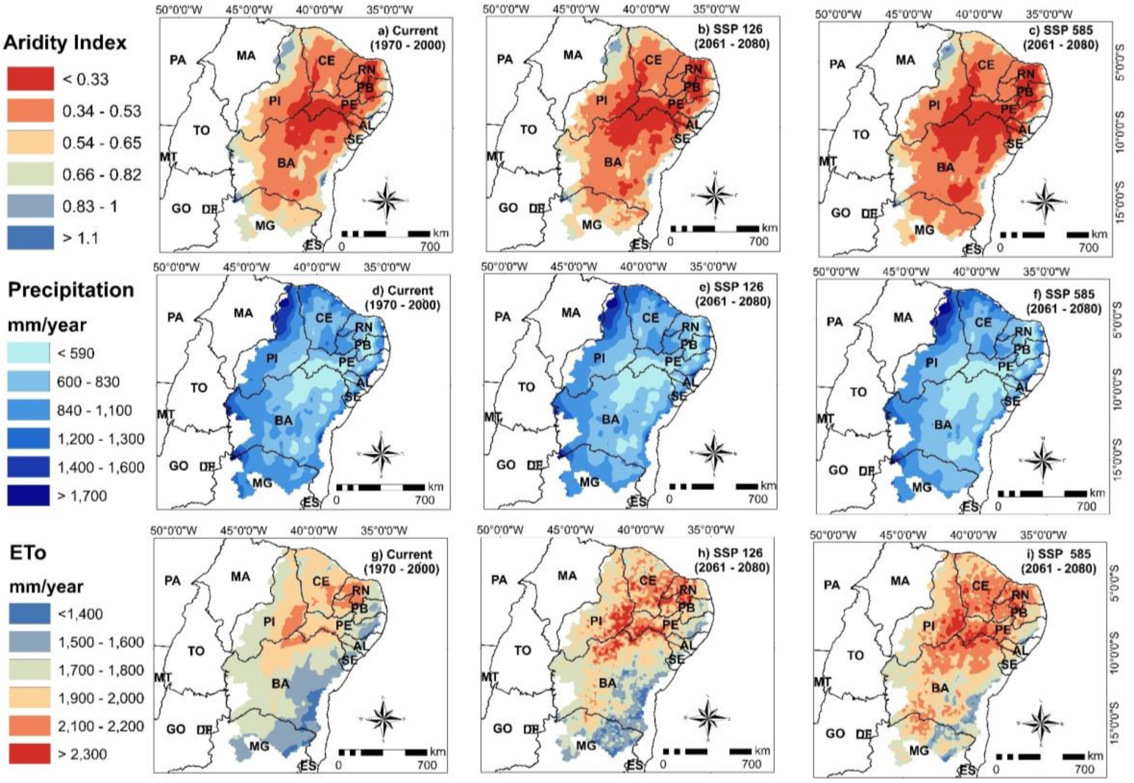

Source: The authors (2023).

Figure 4 - Linear regressions between aridity index (AI), annual precipitation and potential evapotranspiration (ETo) under current conditions and future scenarios for SAB

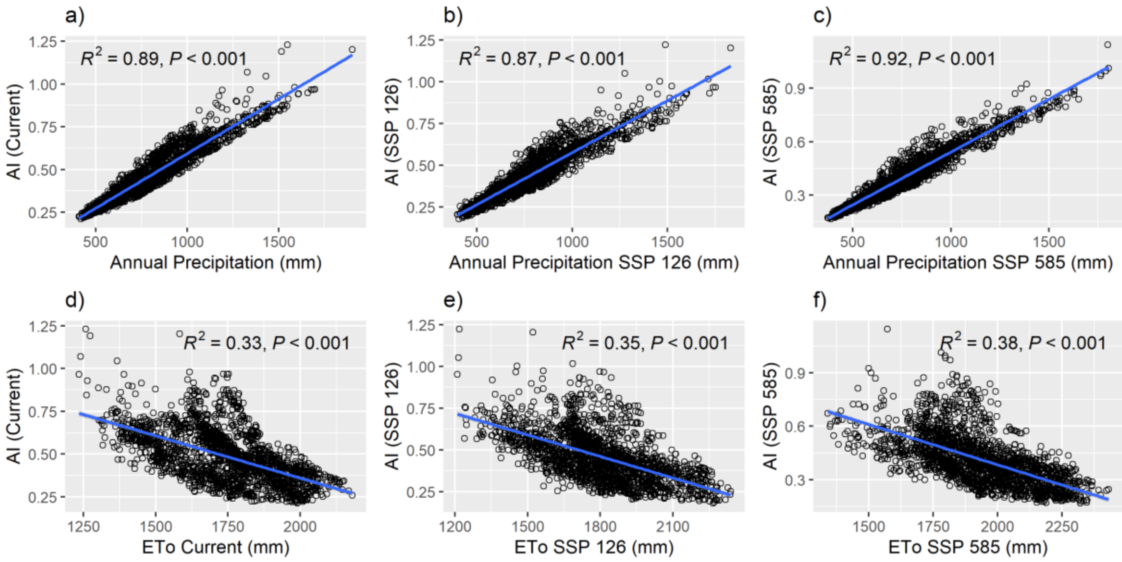

Source: The authors (2023).

Climate classification and climate desertification

Future variations of IA are expected to induce spatial changes in the climate classes in the SAB region (Figure 5). The arid climate condition may expand by 4,100 km² in a more optimistic climate change scenario (SSP 126). This projection is more dramatic in a pessimistic scenario, with an expansion of the arid climate by 21,500 km². The area with the highest recurrence of this expansion in both situations is in the middle part of the SAB, being the semi-arid climate currently predominant (Figure 5 a-f).

Figure 5 – Spatial distribution of climate classes based on Thornthwaite (1948) and areas susceptible to climate desertification for the Brazilian semi-arid region under current conditions (1970 – 2000) and future scenarios (2061 – 2080)

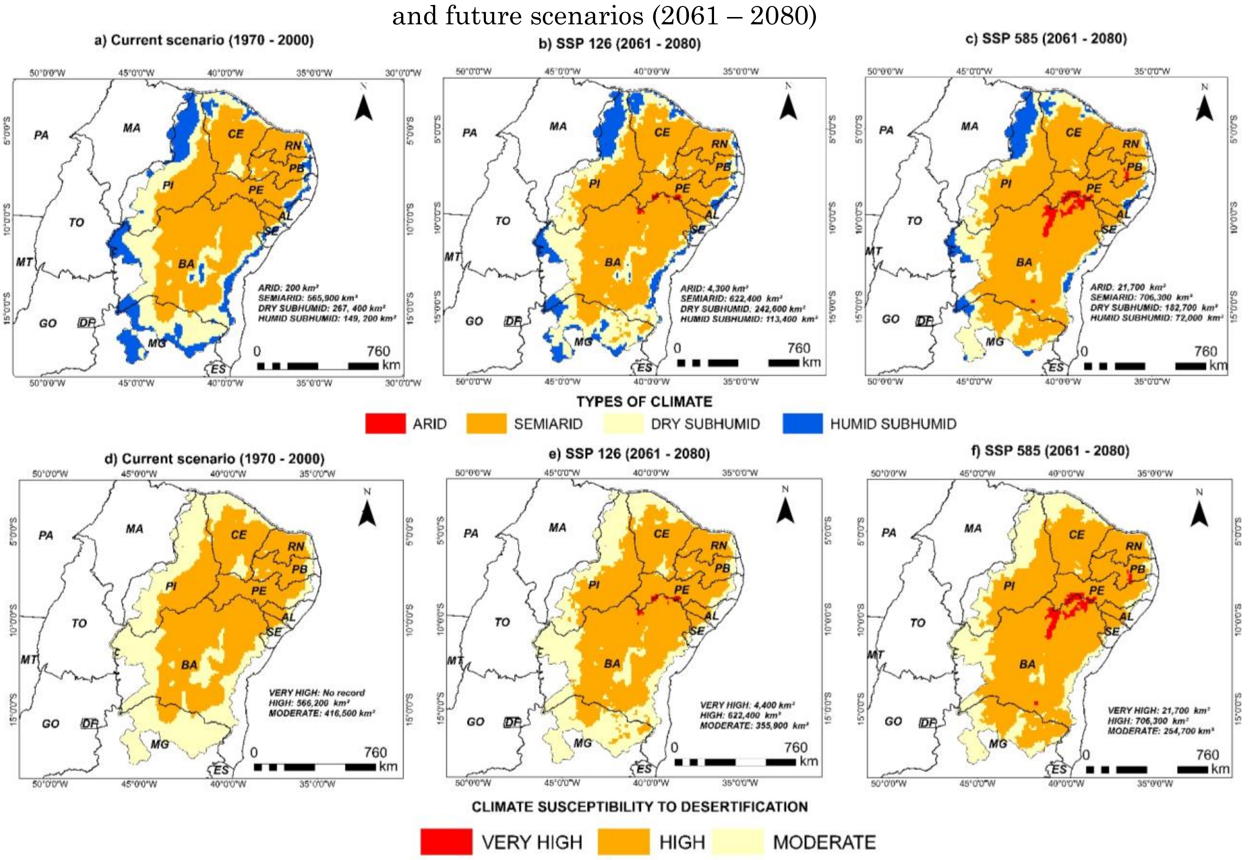

Source: The authors (2023).

Future AI variations should induce spatial changes in the climate classes in the SAB (Figure 5). The arid climate condition may expand by 4,100 km² in a more optimistic climate change scenario (SSP 126). This projection is even more dramatic in a pessimistic scenario, with an arid climate expansion of 21,500 km². The area with the highest recurrence of this expansion in both situations prevails in the middle part of the SAB (Figure 5a, f).

The territorial expansion of arid climate in future scenarios will result from converting zones currently classified as semi-arid (Figure 5). Furthermore, even semi-arid zones should expand over zones of subhumid dry climate. This means that in the current scenario, the semi-arid condition dominates 57.79% of the SAB, in the optimistic scenario 63.34%, while in the most extreme case, 71.87%.

In general, more arid zones amplify the process of susceptibility to desertification. The modeling of this study shows that this behavior is expected in the SAB in the face of climate change (Figure 6a, b). Lands with high susceptibility to climatic desertification will be more frequent in the SAB until the end of the century. Therefore, the expansion of zones of high susceptibility to desertification may increase by 622,400 km² (+10%) in the SSP 126, and more intensely in the SSP 585, increasing by 706,300 km² (+39%).

The expansion of areas with greater susceptibility to climatic desertification should advance over areas with lower levels of susceptibility in the current conditions. Therefore, in the central part of the SAB, zones currently with high susceptibility will be converted to very high susceptibility to desertification in future scenarios (Figure 5), with a territorial expansion of 4,400 in an optimistic scenario (SSP 126) and 21,700 km² in the most extreme climate change scenario (SSP 585). Additionally, the evolution of areas with high susceptibility to desertification should reach even regions to the south (up to 15° S, including the semi-arid region in northern Minas Gerais).

Figure 6 – Sankey graph with the conversions: (a) Climate types in the face of climate change scenarios. (b) Areas susceptible to climate desertification in the face of climate change scenarios

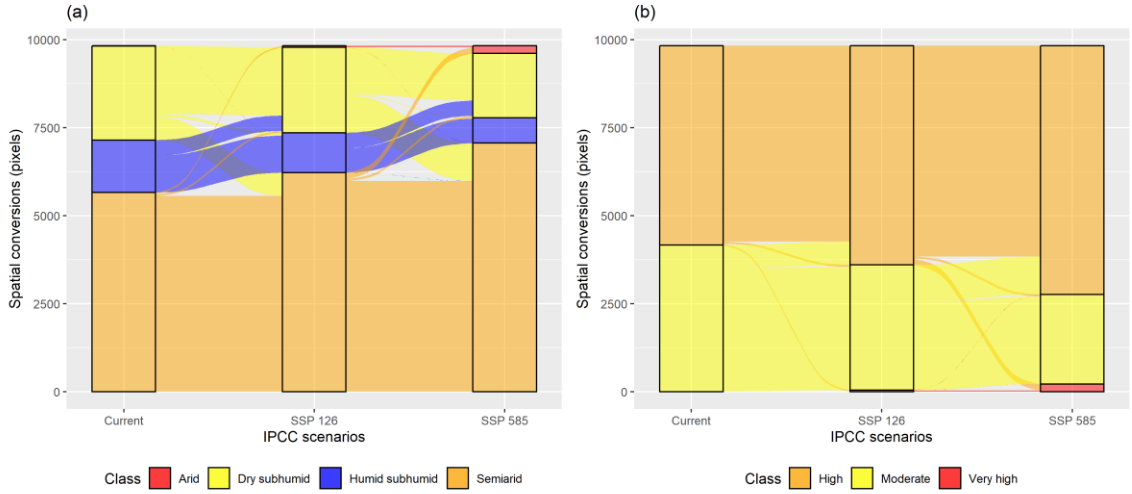

Source: The authors (2023).

DISCUSSION

The study analyzed the effects of climate change on aridity and its impacts on the increase of drylands and the expansion of areas susceptible to climate desertification in the SAB. A crucial step was using precipitation and ETo variables to model aridity indices (AI), a fundamental index to obtain maps of climate classes and levels of climate desertification.

The methodological structure used to model the ETo variable based on machine learning algorithms was highlighted. The Cubist algorithm presented the best performance between the five tested methods, explaining 98% of the distribution of ETo in the SAB (Figure 2). Modeling ETo using these criteria can generate more precise data (ALTHOFF et al., 2020; DIAS et al., 2021).

AI modeling showed that aridity will expand territorially in the SAB (Figure 3). This evidence follows a global trend, as several spatial modeling studies show that aridity is expected to intensify in semi-arid regions (FERNANDEZ et al., 2019; BURRELL; EVANS; DE KAUWE, 2020; DENISSEN et al., 2022). For the SAB, about 23% of the land has desertification nuclei in the current scenario (BEZERRA et al., 2020); therefore, the intensification of aridity conditions and the expansion of dry climates in future scenarios should increase the zones with susceptibility to climate desertification (Figure 5). Earlier studies for South America show a similar pattern, with the expansion of dry climates and the intensification of zones susceptible to desertification (FERNANDEZ et al., 2017; FERNANDEZ et al., 2019).

The central and southern SAB tend to be the most affected by climate desertification in future scenarios: (Figure 5). In the central part, classes with very high susceptibility to desertification will emerge, affecting states in Bahia and part of Pernambuco. These regions already have ongoing desertification processes in the current scenario. Studies in this area show that 45,000 km² of land have become drier in recent decades (SPINONI et al., 2015).

Ranges with high susceptibility to desertification should reach the southern part of the SAB, where the northern region of Minas Gerais is located (Figure 5). These projections align with earlier studies that defined the region as having a high potential for desertification based on the low levels of precipitation and high temperature under current conditions (SANTOS et al., 2022). The implications of increased aridity and desertification can have dramatic consequences in northern Minas Gerais, mainly because it is a densely populated region (1.6 million inhabitants), with a low human development Index (14% below the national average) (IBGE, 2010), and with 25% of the conflicts in the State's rural areas that depend on the productivity of arable land (FERREIRA et al., 2021).

Ecosystem's function will also be affected by the expansion of desertification areas in the SAB. Vegetation with xerophilous characteristics may expand into currently wetter areas (CASTRO OLIVEIRA et al., 2021). The implications of this expansion are changes in the physical environment, such as reduced land cover, loss of nutrients and soil, and changes in the water cycle, further contributing to desertification (ADAMO; CREWS-MEYER, 2006; FAY et al., 2016). Soil loss, for example, has been shown as one of the main indicators of desertification in SAB (PEREZ-MARIN et al., 2012).

The expansion of xerophilous vegetation can negatively affect the region's biodiversity. Studies show that in desertification nuclei, plant species biodiversity decreases (TAVARES et al., 2019). Therefore, it is crucial to consider the effects of climate change and desertification in SAB on the loss of agricultural productivity and biodiversity and soil properties.

FINAL CONSIDERATIONS

Aridity indices, classification of climate classes, and levels of climate desertification were developed for the Brazilian semi-arid region considering climate change scenarios. The results show that the Brazilian semi-arid region may become drier by the end of the century, especially with increased aridity levels and territorial expansion of more arid zones. This dynamic is concerning even in optimistic climate change scenarios (SSP 126).

The intensification of aridity should result in spatial alterations of the climatic classes in the SAB. Dry climates (arid and semi-arid) may expand over areas with wetter climates (sub-humid humid and sub-humid dry).

The intensification of aridity creates zones with high susceptibility to desertification, which will be intensified in the central part of the SAB, and displacement of zones with high susceptibility to desertification towards regions to the south.

ACKNOWLEDGMENTS

To the Fundação de Amparo à Pesquisa do Estado de Minas Gerais (FAPEMIG - Research Support Foundation of the Federal University of Minas Gerais) for the doctoral scholarship (first author). The the Coordenação de Aperfeiçoamento de Pessoal de Nível Superior (CAPES - Coordination for the Improvement of Higher Education Personnel) case number: 88882.315083/2019-01. To the Conselho Nacional de Desenvolvimento Científico e Tecnológico (CNPq - National Council for Scientific and Technological Development) for a productivity grant and postdoctoral scholarship.

REFERENCES

AB'SÁBER, A. N. **Os domínios de natureza no Brasil: potencialidades paisagísticas**. São Paulo: Ateliê Editorial, 2003.

ADAMO, S. B.; CREWS-MEYER, K. A. Aridity and desertification: exploring environmental hazards in Jáchal, Argentina. **Applied Geography**, v. 26, n. 1, p. 61–85, 2006. https://doi.org/10.1016/j.apgeog.2005.09.001.

ALTHOFF, D.; DIAS, S. H. B.; FILGUEIRAS, R.; RODRIGUES, L. N. ETo-Brazil: a daily gridded reference evapotranspiration data set for Brazil (2000–2018). **Water Resources Research**, v. 56, n. 7, p. e2020WR027562., 2020. https://doi.org/10.1029/2020WR027562.

BEZERRA, F. G. S.; AGUIAR, A. P. D. D.; ALVALÁ, R. C. D. S.; GIAROLLA, A., BEZERRA, K. R. A.; LIMA, P. V. P. S.; ARAI, E. Analysis of areas undergoing desertification, using EVI2 multi-temporal data based on MODIS imagery as indicator. **Ecological Indicators**, v. 117, p. 106579, 2020. https://doi.org/10.1016/j.ecolind.2020.106579.

BRUNSON, J. C. Alluvial Plots in ggplot2. 2020.

BURRELL, A. L.; EVANS, J. P.; DE KAUWE, M. G. Anthropogenic climate change has driven over 5 million km2 of drylands towards desertification. **Nature Communications**, v. 11, n. 1, p. 3853, dez. 2020. https://doi.org/10.1038/s41467-020-17710-7.

CASTRO OLIVEIRA, G.; ARRUDA, D. M.; FERNANDES FILHO, E. I.; VELOSO, G. V.; FRANCELINO, M. R.; SCHAEFER, C. E. G. R. Soil predictors are crucial for modelling vegetation distribution and its responses to climate change. **Science of The Total Environment**, v. 780, p. 14668, 2021. https://doi.org/10.1016/j.scitotenv.2021.146680.

DENISSEN, J. M.; TEULING, A. J.; PITMAN, A. J.; KOIRALA, S., MIGLIAVACCA, M.; LI, W.; ORTH, R. Widespread shift from ecosystem energy to water limitation with climate change. **Nature Climate Change**, v. 12, n. 7, p. 677–684, 2022. https://doi.org/10.1038/s41558-022-01403-8.

DIAS, S. H. B.; FILGUEIRAS, R.; FERNANDES FILHO, E. I.; ARCANJO, G. S.; SILVA, G. H. D.; MANTOVANI, E. C.; CUNHA, F. F. D. Reference evapotranspiration of Brazil modeled with machine learning techniques and remote sensing. **Plos one**, v. 16, n. 2, p. e0245834, 2021. https://doi.org/10.1371/journal.pone.0245834.

FAY, P. A.; GUNTENSPERGEN, G. R.; OLKER, J. H.; JOHNSON, W. C. Climate change impacts on freshwater wetland hydrology and vegetation cover cycling along a regional aridity gradient. **Ecosphere**, v. 7, n. 10, p. e01504, 2016. https://doi.org/10.1002/ecs2.1504.

FENG, K., WANG, T.; LIU, S.; KANG, W.; CHEN, X.; GUO, Z.; ZHI, Y. Monitoring desertification using machine-learning techniques with multiple indicators derived from MODIS images in Mu Us Sandy Land, China. **Remote Sensing**, v. 14, n. 11, p. 2663, 2022. https://doi.org/10.3390/rs14112663.

FERNANDEZ, J. P.; FRANCHITO, S. H.; RAO, V. B. Future changes in the aridity of South America from regional climate model projections. **Pure and Applied Geophysics**, v. 176, n. 6, p. 2719–2728, 2019. https://doi.org/10.1007/s00024-019-02108-4.

FERNANDEZ, J. P.; FRANCHITO, S. H.; RAO, V. B.; LLOPART, M. Changes in Koppen–Trewartha climate classification over South America from RegCM4 projections. **Atmospheric Science Letters**, v. 18, n. 11, p. 427–434, 2017. https://doi.org/10.1002/asl.785.

FERREIRA, G. H. C.; OLIVEIRA, B. F.; LAURENTINO, C. M. M. A territorialização camponesa e do agronegócio no Norte de Minas Gerais. **Confins. Revue franco-brésilienne de géographie/Revista franco-brasilera de geografia**, n. 49, 2021. https://doi.org/10.4000/confins.35073.

FICK, STEPHEN E.; HIJMANS, ROBERT J. WorldClim 2: new 1-km spatial resolution climate surfaces for global land areas. **International journal of climatology**, v. 37, n. 12, p. 4302-4315, 2017. https://doi.org/10.1002/joc.5086.

HAUSFATHER, Z.; MARVEL, K.; SCHMIDT, G. A.; NIELSEN-GAMMON, J. W.; ZELINKA, M. Climate simulations: Recognize the 'hot model'problem. Nature, v.605, n.7908, p. 26 – 29, 2022. https://doi.org/10.1038/d41586-022-01192-2.

HUANG, J.; JI, M.; XIE, Y.; WANG, S.; HE, Y.; RAN, J. Global semi-arid climate change over last 60 years. **Climate Dynamics**, v. 46, n. 3, p. 1131–1150, 2016. https://doi.org/10.1007/s00382-015-2636-8.

HUANG, J.; ZHANG, G.; ZHANG, Y.; GUAN, X.; WEI, Y.; GUO, R. Global desertification vulnerability to climate change and human activities. **Land Degradation & Development**, v. 31, n. 11, p. 1380–1391, 2020. https://doi.org/10.1002/ldr.3556.

IBGE. **Censo Demográfico. Rio de Janeiro, Brazil: Fundação Instituto Brasileiro de Geografia e Estatística.** 2010. Available: https://censo2010.ibge.gov.br/resultados.html Access on: Apr. 10, 2022.

KUHN, M.; QUINLAN, R. Cubist: Rule-and instance-based regression modeling. R package version 0.2. 2. 2018.

LIAW, A.; WIENER, M. Classification and regression by randomForest. **R news**, v. 2, n. 3, p. 18–22, 2002.

LIU, Y.; YAO, X.; WANG, Q.; YU, J.; JIANG, Q.; JIANG, W.; LI, L. Differences in reference evapotranspiration variation and climate-driven patterns in different altitudes of the Qinghai–Tibet plateau (1961–2017). **Water**, v. 13, n. 13, p. 1749, 2021. https://doi.org/10.3390/w13131749.

MARQUES DA SILVA, R.; SANTOS, C. A.; ARAÚJO MARANHÃO, K. U.; MEDEIROS SILVA, A.; PORTO DE LIMA, V. R. Geospatial assessment of eco-environmental changes in desertification area of the Brazilian semi-arid region. **Earth Sciences Research Journal**, v. 22, n. 3, p. 175–186, 2018. https://doi.org/10.15446/esrj.v22n3.69904.

MILBORROW, S.; TIBSHIRANI, R. Package 'earth': Multivariate Adaptive Regression Splines. 2019.

MMA, Ministério do Meio Ambiente (MMA). P rograma de Ação Nacional de Combate à De sertificação e Mitigação dos Efeitos da Seca: PANBRASIL. Edição Comemorativa dos 10 a nos da Convenção das Nações Unidades de Combate à Desertificação e Mitigação dos Efeit os da Seca – CCD. Brasília: MMA, 2004. 225p.

MUTTI, P. R.; ABREU, L. P.; MB ANDRADE, L.; SPYRIDES, M. H. C.; LIMA, K. C.; DE OLIVEIRA, C. P.; BEZERRA, B. G. A detailed framework for the characterization of rainfall climatology in semi-arid watersheds. **Theoretical and Applied Climatology**, v. 139, n. 1–2, p. 109–125, 2020. https://doi.org/10.1111/tgis.12926.

PEREZ-MARIN, A. M.; CAVALCANTE, A. D. M. B.; MEDEIROS, S. S.; TINÔCO, L. D. M.; SALCEDO, I. H. Núcleos de desertificação no semiárido brasileiro: ocorrência natural ou antrópica. **Parcerias Estratégicas**, v. 17, n. 34, p. 87-106, 2012.

POZO, A. D.; BRUNEL-SALDIAS, N.; ENGLER, A.; ORTEGA-FARIAS, S.; ACEVEDO-OPAZO, C.; LOBOS, G. A.; MOLINA-MONTENEGRO, M. A. Climate change impacts and adaptation strategies of agriculture in Mediterranean-climate regions (MCRs). **Sustainability**, v. 11, n. 10, p. 2769, 2019. https://doi.org/10.3390/su11102769.

RODRIGUEZ, P. P.; GIANOLA, D. BRNN: Bayesian regularization for feed-forward neural networks. **R package version 0.6**, 2016.

SANTOS, N. O.; MACHADO, R. A. S.; GONZÁLEZ, R. C. L. Identification of levels of anthropization and its implications in the process of desertification in the Caatinga biome (Jeremoabo, Bahia-Brazil). **Cuadernos de Investigación Geográfica**, v. 48, n. 1, p. 41-57, 2022. https://doi.org/10.1002/joc.4124.

SANZHEEV, E. D.; MIKHEEVA, A. S.; OSODOEV, P. V.; BATOMUNKUEV, V. S.; TULOKHONOV, A. K. Theoretical approaches and practical assessment of socio-economic effects of desertification in Mongolia. **International Journal of Environmental Research and Public Health**, v. 17, n. 11, p. 4068, 2020. https://doi.org/10.3390/ijerph17114068.

SILVA, L. A. P.; SOUZA, C. M. P.; SILVA, C. R.; FILGUEIRAS, R.; SENA-SOUZA, J. P.; FERNANDES-FILHO, E. I.; LEITE, M. E. Mapping the effects of climate change on reference evapotranspiration in future scenarios in the Brazilian Semi-arid Region - South America. **Revista Brasileira de Geografia Física**, v. 16, p. 1001-1012, 2023. https://doi.org/10.26848/rbgf.v16.2.p1001-1012

SOUZA, C. M. P. D.; THOMAZINI, A.; SCHAEFER, C. E. G. R.; VELOSO, G. V.; MOREIRA, G. M.; FERNANDES FILHO, E. I. Multivariate analysis and machine learning in properties of Ultisols (Argissolos) of Brazilian Amazon. **Revista Brasileira de Ciência do Solo**, v. 42, 2018. https://doi.org/10.1590/18069657rbcs20170419.

SPINONI, J.; VOGT, J.; NAUMANN, G.; CARRAO, H.; BARBOSA, P. Towards identifying areas at climatological risk of desertification using the Köppen–Geiger classification and FAO aridity index. **International Journal of Climatology**, v. 35, n. 9, p. 2210-2222, 2015. https://doi.org/10.1002/joc.4124

TAVARES, V. C.; DE ARRUDA, Í. R. P.; DA SILVA, D. G. Desertificação, mudanças climáticas e secas no semiárido brasileiro: uma revisão bibliográfica. **Geosul**, v. 34, n. 70, p. 385–405, 2019. https://doi.org/10.5007/2177-5230.2019v34n70p385.

TEAM, R. C. R: A language and environment for statistical computing. R Foundation for Statistical Computing, Vienna, Austria. Available: http://www.R-project.org/. Access on: Jan. 05, 2022.

THORNTHWAITE, C. W. An approach toward a rational classification of climate. **Geographical review**, v. 38, n. 1, p. 55–94, 1948. https://doi.org/10.2307/210739.

UNEP. United Nations Environmental Programme, **World Atlas of Desertification**, London: Ed. Edward Arnold Publishers, 1992.

VERGARA, W. L. GALLARDO LOMELI, M. FRANCO CHUAIRE, S. Initiative 20X20: A landscape restoration movement rises in Latin America restoration enhance regeneration of seasonal deciduous and the Caribbean**. World Resources Institute**, 2015. Available https://www.wri.org/insights/initiative-20x20-landscape-restoration-movement-rises-latin-america-and-caribbean. Acess on: Jan. 05, 2022.

VIEIRA, R. M. D. S. P.; SESTINI, M. F.; TOMASELLA, J.; MARCHEZINI, V.; PEREIRA, G. R.; BARBOSA, A. A.; OMETTO, J. P. H. B. Characterizing spatio-temporal patterns of social vulnerability to droughts, degradation and desertification in the Brazilian northeast. **Environmental and Sustainability Indicators**, v. 5, p. 100016, 2020. https://doi.org/10.1016/j.indic.2019.100016.

VIEIRA, R. M. D.S.P; TOMASELLA, J.; BARBOSA, A. A.; MARTINS, M. A.; RODRIGUEZ, D. A.; REZENDE, F. S.; SANTANA, M. D. Desertification risk assessment in Northeast Brazil: Current trends and future scenarios. **Land Degradation & Development**, v. 32, n. 1, p. 224–240, 2021. https://doi.org/10.1002/ldr.3681.

WU, Y.; ZHANG, X.; LI, C.; XU, Y.; HAO, F.; YIN, G. Ecosystem service trade-offs and synergies under influence of climate and land cover change in an afforested semi-arid basin, China. **Ecological Engineering**, v. 159, p. 106083, 2021. https://doi.org/10.1016/j.ecoleng.2020.106083.

ZARCH, M. A. A.; SIVAKUMAR, B.; MALEKINEZHAD, H.; SHARMA, A. Future aridity under conditions of global climate change. **Journal of Hydrology**, v. 554, p. 451-469, 2017. https://doi.org/10.1016/j.jhydrol.2017.08.043.

ZHOU, S.; WILLIAMS, A. P.; LINTNER, B. R.; BERG, A. M.; ZHANG, Y.; KEENAN, T. F.; GENTINE, P. Soil moisture–atmosphere feedbacks mitigate declining water availability in drylands. **Nature Climate Change**, v. 11, n. 1, p. 38–44, 2021. https://doi.org/10.1038/s41558-020-00945-z.

AUTHORS CONTRIBUTION

Lucas Augusto Pereira da Silva conceived the study, set up the database, software, analyzed the data and wrote the original text. Claudionor Ribeiro da Silva conceived and supervised the study. Cristiano Marcelo Pereira de Souza performed the formal analyzes and revised the text. Édson Luís Bolfe, João Paulo Sena Souza and Marcos Esdras Leite revised the text.